

Hydrogen internal-friction peak and interaction of dissolved interstitial atoms in Nb and Ta

M. S. Blanter

Moscow Instrumental Institute, Stromynka 20, Moscow 107846, Russia

(Received 2 December 1992; revised manuscript received 1 November 1993)

Internal friction due to diffusion of H and D atoms under stress was calculated for Ta(Nb)-H(D)-O(N) alloys. The long-range strain-induced (elastic) interaction was supplemented by a repulsive interaction in the nearest coordination shells due to a screened Coulomb interaction between charged interstitials. Short-range order in the interstitial solid solution was simulated by the Monte Carlo method. It was suggested that the interatomic interaction affects internal friction by changing the arrangement and the energy of H or D atoms in solid solution and therefore the activation energy of the relaxation process. Computer simulation was carried out with calculated values of energies of elastic interaction and with different radii of additional repulsive interaction. The calculated spectra are in good agreement with experimental data when the repulsive interaction extends out to the third coordination shell. The strain-induced interaction model, when supplemented by repulsion in the three nearest shells, is a useful description of these solid solutions.

I. INTRODUCTION

The interaction of solute atoms in metals has been the subject of numerous experimental studies because such information is indispensable for understanding many basic physical processes such as short-range order, segregation, ordering, diffusion, etc. The interaction energies are necessary for calculations of phase equilibria and phase diagrams, and the mechanical and physical properties of solid solutions.

The theory of solute interactions is yet imperfectly developed and it is so far impossible to obtain these energies. However, the more limited theory of strain-induced (elastic) interaction in the framework of the model of a discrete crystal lattice has been developed¹ and the energies of the pair interactions of H, D, O, N, and C in bcc metals (V, Nb, Ta, Cr, Mo, W, and α -Fe) evaluated.²⁻⁶ The interaction is strong and long range.

Calculations^{7,8} of atomic structure in interstitial solid solutions with a long-range order, based on V, Nb, Ta, and α -Fe, performed with the calculated energies of the strain-induced interaction, showed that the interaction determines, in general, the structure of such solid solutions. However, the calculations showed¹ also that it is necessary to supplement the long-range elastic interaction by a short-range repulsion of interstitials. In the case of the H-H interaction, the existence of this repulsion is evident from analysis of hydride structures.⁹

A possible source of the repulsion is the screened Coulomb interaction of charged interstitials.³ Rough estimations of the energies of this interaction were carried out for H-H pairs in Nb,³ but for further progress it is necessary to find methods for investigation of the interaction. It is known that internal friction spectra of solid solutions are connected with the solute interaction.^{10,11} However, internal friction is usually used to get qualitative information or rough estimations of the interaction

energy. These estimations are not adequate for calculations of the structure and properties of solid solutions.

More accurate data can be obtained by the method of computer simulation of internal friction spectra taking into account the concrete energies of the solute interaction. This method has been used for investigation of the interatomic interaction in Ta-O (Ref. 12) and Nb-V-O (Ref. 13) alloys.

In this paper the internal friction due to "diffusion under stress" of H and D atoms near O or N atoms in Nb and Ta was calculated taking into account the calculated energies of the long-range strain-induced interaction and varying the radius of the screened Coulomb repulsion. The purpose was (a) to determine the radius of the repulsion, (b) to verify the applicability of the applied model of the solute interaction, and (c) to refine the relaxation mechanism.

II. INTERACTION ENERGIES

As mentioned above, the model of H-H, D-D, O-H, O-D, N-H, and N-D interactions is a long-range elastic interaction supplemented by a screened Coulomb interaction in the nearest coordination shells. The calculation of the H-H Coulomb interaction in Nb (Ref. 3) and an analysis of hydride structures⁹ showed that this interaction is repulsive. However, there is no information about the O(N)-H(D) Coulomb interaction. According to an electrotransport experiment, oxygen has a positive effective charge in Nb and Ta (Ref. 14) similar to hydrogen, suggesting that the H(D)-O(N) screened Coulomb interaction is also repulsive.

The energies of the strain-induced pair interaction of interstitials calculated within the model of a discrete crystal lattice were taken from previous papers³⁻⁵ or calculated in the present paper based on the data from the

TABLE I. Values of the concentration coefficients of the expansion of the crystal lattices u_{11} and u_{33} .

Metal	Nb			Ta			
	O	N	H and D	O	N	H	D
u_{11}	-0.06	-0.08	+0.058	-0.04	-0.05	+0.052	+0.048
u_{33}	+0.50	+0.60	+0.058	+0.47	+0.56	+0.052	+0.048

papers mentioned above. The description of the calculation method can be found in Khachatryan's book.¹

The following parameters were used in the calculations:

(i) u_{11} and u_{33} are the coefficients of expansion of the crystal lattice per unit concentration. They describe distortions created by the interstitials. For octahedral interstices (oxygen and nitrogen atoms) u_{11} is not equal to u_{33} and for tetrahedral interstices (hydrogen and deuterium atoms) $u_{11} = u_{33}$. (ii) The Born-von Karman constants were used for a description of the elastic behavior of the crystal lattice.

The reported energies of the elastic interaction³⁻⁵ were corrected by taking into account new more precise values of u_{11} and u_{33} (Table I). For oxygen and nitrogen, u_{11} and u_{33} were found from the concentration dependence of the lattice parameters and the Snoek relaxation intensity of solid solution,² for hydrogen and deuterium from the concentration dependence of the volume of the solid solution.¹⁵

The energies $W(\mathbf{r}_i - \mathbf{r}_j)$ of the strain-induced pair interactions of interstitials located in tetrahedral interstices can be expressed as²

$$W(\mathbf{r}_i - \mathbf{r}_j) = u_{33}^2 A(\mathbf{r}_i - \mathbf{r}_j), \quad (1)$$

and those of two atoms when one is located in an octahedral interstice and the other is located in a tetrahedral interstice (O-H, O-D, N-H, and N-D pairs) can be expressed as

$$W(\mathbf{r}_i - \mathbf{r}_j) = u_{33}^{(o)} u_{33}^{(t)} [B(\mathbf{r}_i - \mathbf{r}_j) + G(\mathbf{r}_i - \mathbf{r}_j)t], \quad (2)$$

TABLE II. Energies (eV) of the strain-induced pair interaction of interstitials located in tetrahedral interstices $\mathbf{r}_i = 4(201)a_0$ and \mathbf{r}_j .

$\frac{4(\mathbf{r}_i - \mathbf{r}_j)}{a_0}$	Number of coord. shells	$\frac{ \mathbf{r}_i - \mathbf{r}_j }{a_0}$	Energies		
			H-H and D-D in Nb	H-H in Ta	D-D in Ta
101	1	0.35	-0.295	-0.244	-0.208
200	2	0.5	-0.186	-0.168	-0.143
211	3	0.61	-0.097	-0.101	-0.086
220	4	0.71	-0.053	-0.048	-0.041
301	5	0.79	-0.037	-0.036	-0.031
222	6	0.87	-0.020	-0.016	-0.014
321	7	0.94	+0.011	+0.009	+0.008
004	8a	1	-0.017	-0.013	-0.011
400	8b	1	+0.037	+0.016	+0.014
330	9a	1.06	+0.050	+0.043	+0.036
141	9b	1.06	+0.054	+0.049	+0.042
402	10a	1.12	-0.005	-0.004	-0.003
042	10b	1.12	+0.071	+0.063	+0.053
332	11	1.17	+0.001	-0.004	-0.003
422	12	1.22	-0.003	+0.003	+0.002

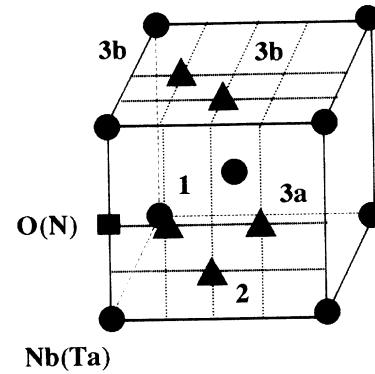


FIG. 1. Disposition of tetrahedral interstices around O or N atoms.

where $u_{33}^{(o)}$ and $t = u_{11}^{(o)}/u_{33}^{(o)}$ stand for atoms located in octahedral and $u_{33}^{(t)}$ in tetrahedral interstices. The vectors \mathbf{r}_i and \mathbf{r}_j show the positions of the atoms of the pair. $A(\mathbf{r}_i - \mathbf{r}_j)$, $B(\mathbf{r}_i - \mathbf{r}_j)$ and $G(\mathbf{r}_i - \mathbf{r}_j)$ are universal coefficients which are valid for any interstitial solid solution for a given host lattice.

The coefficients $A(\mathbf{r}_i - \mathbf{r}_j)$ were evaluated using data for Nb (Ref. 3) and for Ta (Ref. 5), as were $B(\mathbf{r}_i - \mathbf{r}_j)$ and $G(\mathbf{r}_i - \mathbf{r}_j)$ for Nb and Ta.⁴ The energies displayed in Tables II and III were determined by substitution of these coefficients and the values of u_{11} and u_{33} (see Table I) in Eqs. (1) and (2). The disposition of the tetrahedral interstices in the nearest coordination shells of an octahedral interstice is shown in Fig. 1.

Positive values of the interaction energy $W(\mathbf{r}_i - \mathbf{r}_j)$ mean repulsion. One can see in the tables that this interaction is strong, long range, and anisotropic. In all cases the elastic interaction is strongly attractive at the nearest distances up to the third coordination shell.

The Coulomb repulsion was taken into account by suppression of the elastic attraction in the nearest coordination shells. We used different radii of the repulsion and

TABLE III. Energies (eV) of the strain-induced pair interaction of interstitials, one located in the octahedral interstice $\mathbf{r}_i = 2(001)a_0$ (O or N atoms) and the other in the tetrahedral interstice \mathbf{r}_j (H or D atoms).

$\frac{4(\mathbf{r}_i - \mathbf{r}_j)}{a_0}$	Number of coord. shell	$\frac{ \mathbf{r}_i - \mathbf{r}_j }{a_0}$	Energies					
			in Nb		in Ta			
			O-H(D)	N-H(D)	O-H	N-H	O-D	N-D
100	1	0.25	-0.73	-0.94	-0.80	-0.94	-0.74	-0.87
201	2	0.56	-0.29	-0.39	-0.33	-0.39	-0.30	-0.36
300	3a	0.75	-0.12	-0.18	-0.15	-0.17	-0.14	-0.16
212	3b	0.75	-0.064	-0.12	-0.087	-0.10	-0.08	-0.09
230	4	0.90	+0.08	+0.094	+0.068	+0.081	+0.063	+0.075
232	5a	1.03	-0.025	-0.021	-0.018	-0.021	-0.017	-0.019

calculated energies of O(N)-H(D), H-H, and D-D interaction (see Tables II and III) for calculation of the internal friction spectra. The radii of the Coulomb repulsion were obtained by comparing the cases of coincidence of the calculated spectra with the experimental ones. When the Coulomb repulsion radii were obtained, the energies of the elastic interaction outside these radii could be used for calculation of the structure and properties of solid solutions.

III. CALCULATION METHOD

It is known that the "hydrogen Snoek-type maximum" appears due to diffusion under stress of H or D atoms near immobile O or N atoms. For calculation of the internal friction taking into account the solute interaction, the following assumptions were made.

(i) The long-range interaction of interstitials affects the arrangement of H and D atoms [creates O(N)-H(D) pairs and short-range order of hydrogen and deuterium atoms] and changes the energy of H and D atoms in tetrahedral interstices by ΔE_p and consequently changes the individual diffusion barrier H_p of the p th hydrogen or deuterium atom.

(ii) The preexponential factor τ_0 of the relaxation time τ is independent of the solute interaction. This assumption is supported by the fact that the values of τ_0 of identical relaxation processes are in close agreement in different solid solutions and that τ_0 of the Snoek relaxation depends only slightly on substitutional atoms.¹⁶

(iii) Contributions to the internal friction are created by H and D atoms in the first four coordination shells around O and N atoms (the distance of the strongest attractive interaction).

Thus calculation of the internal friction was performed in two stages: (a) Monte Carlo computer simulation of the arrangement of mobile H or D atoms in the model crystal with immobile O or N atoms taking into account the pair H(D)-H(D) and O(N)-H(D) interaction, with determination of the energy ΔE_p of each H or D atom in the potentials of other interstitials; (b) for each p th H or D atom located near fixed O or N atoms its contribution to the internal friction was obtained according to its activation energy H_p .

A. Monte Carlo simulation

To calculate short-range order and ΔE_p a computer Monte Carlo simulation was carried out. H or D atoms were randomly placed into tetrahedral interstices of a $(12 \times 12 \times 12)a_0^3$ (a_0 is the lattice parameter of the host lattice) bcc crystal with periodic boundary conditions. Isolated fixed oxygen or nitrogen atoms were also placed in octahedral interstices periodically.

The Hamiltonian of the system is equal to the sum of all pair interaction energies

$$\kappa = (1/2) \left[\sum_{i,j} W(\mathbf{r}_i - \mathbf{r}_j) C(\mathbf{r}_i) C(\mathbf{r}_j) + \sum_{i,m} W(\mathbf{r}_i - \mathbf{r}_m) C(\mathbf{r}_i) \right], \quad (3)$$

where \mathbf{r}_i and \mathbf{r}_j are positions of tetrahedral interstices, and \mathbf{r}_m are positions of fixed oxygen or nitrogen atoms. $W(\mathbf{r}_i - \mathbf{r}_j)$ are pairwise (D-D) or (H-H) interaction energies; $W(\mathbf{r}_i - \mathbf{r}_m)$ are pairwise H(D)-O(N) interaction energies. $C(\mathbf{r}_i)$ are the occupation numbers for tetrahedral interstices. $C(\mathbf{r}_i) = 1$ if the interstice is occupied, $C(\mathbf{r}_i) = 0$ otherwise.

A mobile H or D interstitial and one of its four neighboring tetrahedral interstices were randomly chosen at a constant temperature. When the chosen interstice was empty, the Hamiltonian difference $\Delta \kappa$ of the corresponding jump was calculated. The jump was allowed if either $\Delta \kappa$ happened to be negative or the probability of the jump $\varphi = \exp(-\Delta \kappa/kT)$ was greater than a certain random number $0 < x < 1$ (k is the Boltzmann constant). After multiple repetition of the process some steady short-range order configurations were obtained.

For the atomic configuration, the p th atom located in the tetrahedral interstice has an energy of interaction, ΔE_p , with other interstitials, fixed and mobile, equal to

$$\Delta E_p = \sum_j W(\mathbf{r}_p - \mathbf{r}_j) C(\mathbf{r}_j) + \sum_m W(\mathbf{r}_p - \mathbf{r}_m). \quad (4)$$

B. Calculation of internal friction

The contribution of the p th H or D atom is expressed by the Debye equation with the activation energy H_p ,

TABLE IV. Parameters of diffusion (Ref. 17) and preexponential factor τ_0 .

Metal	Nb		Ta	
	H	D	H	D
Diffusing species				
H_D (eV)	0.068	0.127	0.040	0.160
D_0 (10^{-4} cm ² s ⁻¹)	0.9	5.2	0.02	4.6
τ_0 (10^{-13} s)	1.68	0.29	75.6	0.33

$$H_p = H_D - \Delta E_p, \quad (5)$$

where H_D is equal to the activation energy of diffusion of an interstitial atom. We neglected the change of energy of the saddle point of the diffusion barrier according to calculations for Ta-O.¹²

Then at a given temperature T the internal friction Q^{-1} can be calculated summing up all interstitial contributions

$$Q^{-1} = \frac{\Delta}{T} \sum_{p=1}^N \frac{\omega \tau_p}{1 + (\omega \tau_p)^2}, \quad (6)$$

where N is the number of H or D atoms, $\omega = 2\pi f$ is the angular frequency of vibration, τ_p is the relaxation time of the p th atom, Δ is the relaxation strength, and T is absolute temperature, and further

$$\tau_p = \tau_0 \exp(H_p/kT). \quad (7)$$

Dividing Δ by T takes into account the well-known temperature dependence of the relaxation strength.

H_D and τ_0 were taken according to diffusion data¹⁷ obtained from the Gorsky effect. For diffusion through tetrahedral interstices of the bcc lattice¹⁰

$$\tau_0 = \frac{a_0^2}{72D_0}, \quad (8)$$

where D_0 is the preexponential factor of the diffusion coefficient. The values of H_D , D_0 , and τ_0 used in this paper are shown in Table IV. The internal friction Q^{-1} was calculated at each temperature by averaging Q^{-1} over the atomic configurations obtained from the Monte Carlo simulation.

IV. RESULTS AND DISCUSSION

We know experimental data on the hydrogen Snoek-type maximum for seven Nb(Ta)-H(D)-O(N) systems of eight possible. For three of these systems—Nb-H-O, Nb-D-O, and Ta-H-O—we have experimental data over wide ranges of frequency and temperature. For the other systems (except Nb-D-N), data are available only for one frequency. We have detailed experimental data for Nb-H-O alloys and therefore we would like to describe the results of a computer simulation for this alloy in detail.

A. Nb-H-O alloys

Preliminary analysis was performed for $f = 1$ Hz. At $f = 0.76$ Hz the experimental temperature of the hydrogen maximum in Nb is 50 K.¹⁸ Experimental data were taken for specimens with different concentrations of “light” and “heavy” interstitials; the temperature of the hydrogen Snoek-type maximum is almost independent of concentration but its height depends upon the concentration. A preliminary simulation of Nb-H-O alloys in wide ranges of H (0.09–0.38 at. %) and O (0.23–1.85 at. %) concentration showed that the calculated peak temperature is also independent of concentration. Therefore, all results in this paper are given for one level of concentrations (0.26 at. % of H or D and 0.8 at. % of O or N).

The results of the computer simulation of the internal friction spectra in the range of 30–80 K are shown for different radii of H-H and H-O repulsions in Table V. When the repulsion is not taken into consideration there are no internal friction maxima in the temperature range. The absence of peaks is caused by too high values of ΔE_p and consequently H_p ; if the maximum does appear, its temperature is much higher than the experimental one. Internal friction maxima are also absent when the H-O repulsion expands out to the third-b coordination shell. In this case the H-O elastic attraction is too weak to hold hydrogen near oxygen and therefore $Q^{-1} = 0$.

For H-O repulsion in the two or three nearest shells and for H-H repulsion in the three nearest shells, a maximum appears as in the experiments. A weak additional peak appears at higher temperatures in the calculated spec-

TABLE V. Calculated internal friction spectra of Nb-H-O alloys (30–80 K, $f = 1$ Hz).

		H-O interaction				
		Radius of repulsion (coord. shell number)				
		Without repulsion	1	2	3a	3b
H-H interaction	Without repulsion	No peaks	No peaks	No peaks	No peaks	No peaks
radius of repulsion (coord. shell number)	1	No peaks	No peaks	No peaks	No peaks	No peaks
	2	No peaks	No peaks	No peaks	No peaks	No peaks
	3	No peaks	No peaks	One peak at 74 K	One peak at 56 K	No peaks
	4	No peaks	No peaks	Two peaks	One peak at 56 K	No peaks
	5	No peaks	No peaks	Three peaks	One peak at 56 K	No peaks

TABLE VI. Calculated and experimental parameters of hydrogen Snoek-type maxima.

Parameter	Version of potentials	Nb-H-O	Nb-D-O	Ta-H-O
T_p (K) at $f=1000$ Hz	A	104	128	127
	B	74	98	87
	Experiment	79	106	77
T_p (K) at $f=10000$ Hz	A	118	140	152
	B	83	111	101
	Experiment	93	120	88
H_{eff} (eV)	A	0.19	0.25	0.18
	B	0.145	0.17	0.13
	Experiment	0.135	0.17	0.12
τ_0 (s)	A	1.1×10^{-13}	1.8×10^{-14}	1.4×10^{-11}
	B	1.8×10^{-14}	2.0×10^{-13}	3.7×10^{-12}
	Experiment	8.5×10^{-13}	9.9×10^{-13}	1.4×10^{-12}
References for experimental data		20, 21	21, 22	20

trum, similar to a peak noted in some experiments.¹⁸ Generally, one can conclude in those cases that the calculated spectrum is in qualitative agreement with the experimental spectrum. There is quantitative agreement only for H-O repulsion out to the third-a shell and H-H repulsion out to at least the third shell. In this case the calculated temperature (56 K) is in good agreement with

the experiment (50 K).

The shortest radius of the H-H repulsive interaction (three shells) found necessary for agreement of the calculated and experimental spectra is in good agreement with data obtained from the structure of hydrides.⁹

For analysis in a wide range of temperatures and frequencies we have used two versions of the potentials: the H-O repulsive interaction in shells 1 and 2 (version A) and in shells 1, 2, and 3a (version B). H-H repulsion was taken in the three nearest shells. The results are shown in Fig. 2 and Table VI. One can see that both calculated and experimental data are described by the usual dependence of the temperature of maximum T_p on frequency,¹¹

$$\ln f = -\ln(2\pi\tau_0) - \frac{H_{\text{eff}}}{kT_p}, \quad (9)$$

where H_{eff} is the effective energy of the relaxation process.

All the experimental data shown in Table VI were obtained from the curves numbered 3 in Fig. 2. The results of calculations for Nb-H-O with version B are in good agreement with the experimental results over a wide range of frequencies. Version A is much farther off.

It is interesting to note that the calculated spectrum is not determined by the value of the highest energy of the H-O attraction after compensation of the elastic attraction in the nearest shells. For potentials of version B this value is equal to -0.064 eV in the 3b shell. We calculated internal friction using the value -0.064 eV in shells 1, 2, 3a, and 3b (Fig. 1), each in its turn without attraction in the rest of these shells. The temperature of the peak was in an agreement with the experimental one only for shell 3b. This means that the axis of the H-O pair in Nb is close to the [111] direction but not to [100]. Therefore, we can observe the peak in monocrystals when an alternating load is applied in the [111] direction but not in the [100] one. The result is confirmed by experiment.¹⁹ Figure 1 also shows that during the relaxation process the hydrogen atom can move from one tetrahedral interstice in shell 3b around an oxygen atom to another tetrahedral interstice in the same shell.

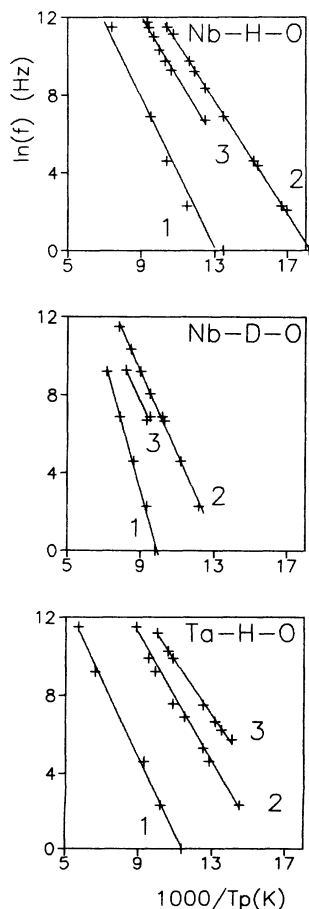


FIG. 2. Frequency dependence of hydrogen Snoek-type peak temperature T_p . 1 and 2, calculated with potentials of versions A and B, respectively; 3, experimental.

B. Other alloys

A computer simulation of the internal friction of Nb-D-O and Ta-H-O alloys (Fig. 2 and Table VI) for which we have experimental data in a wide frequency range confirmed the results for Nb-H-O alloys. The use of version A of potentials gives results which do not coincide with the experiment. When we used version B, the calculated temperatures of the peaks and the effective activation energies of the relaxation process were in good agreement with the experiment. Increase of the repulsion radius of O-H(D) pairs out to shell 3b results in the absence of the peak.

Thus, in all three investigated systems, Nb-H-O, Nb-D-O, and Ta-H-O, the repulsive interaction is essential up to shell 3a and the model of strain-induced interaction of H-H(D-D) and O-H(D) atoms supplemented by such repulsive interaction is useful for description of the internal friction due to diffusion under stress of H and D atoms.

It is interesting to observe that although the calculated effective activation energy H_{eff} is close to the sum of the activation energy of diffusion of H or D atoms and the maximum energy of attraction of O and H(D) atoms (in shell 3b), it is not equal to this sum. For Nb-D-O alloys the difference is equal to 0.02 eV, for Nb-H-O -0.012 eV. The results show that internal friction is governed not only by the maximum interaction energy but also by the interaction involving several coordination shells.

As for the other four alloy systems, the computer simulation was made with the use of only version B of potentials (Table VII). One can see that in three cases (Nb-H-N, Ta-H-N, Ta-D-O) the calculated temperature

TABLE VII. Comparison of calculated and experimental temperatures of internal friction maxima.

Alloys	f (Hz)	T_p (K)	
		Calculated	Experimental
Nb-H-N	0.76	65	60 ^a
Ta-H-N	0.61	63	50 ^b
Ta-D-O	20000	143	126 ^c
Ta-D-N	0.76	98	65 ^b

^aReference 23.

^bReference 24.

^cReference 25.

of the internal friction peak is in good agreement with experiment. In one case (Ta-D-N) the difference is considerable but that does not mean that the model of the interatomic interaction is not useful for a description of these solid solutions.

V. CONCLUSIONS

(1) The spectra of internal friction due to diffusion under stress of interstitial atoms in bcc metals are very sensitive to interatomic interaction energies.

(2) The long-range strain-induced (elastic) energies of the H-H(D-D) and O(N)-H(D) interactions, supplemented by a repulsive interaction in the nearest coordination shells, are useful for a description of the solid solutions.

(3) The repulsive interaction of interstitial atoms in bcc metals extends up to the third coordination shell.

¹ A. G. Khachaturyan, *Theory of Structural Transformations in Solids* (Wiley, New York, 1983).

² M. S. Blanter and A. G. Khachaturyan, *Metall. Trans. A* **9**, 753 (1978).

³ V. G. Vaks, N. E. Zein, V. Zinenko, and A. G. Orlov, *Zh. Eksp. Teor. Fiz.* **87**, 2030 (1984) [*Sov. Phys. JETP* **60**, 1171 (1984)].

⁴ A. I. Shirley, C. K. Hall, and N. J. Prince, *Acta. Metall.* **31**, 985 (1983).

⁵ H. Horner and H. Wagner, *J. Phys. C* **7**, 3305 (1974).

⁶ M. S. Blanter, *Fiz. Met. Metalloved.* **60**, 50 (1985).

⁷ M. S. Blanter and A. G. Khachaturyan, *Phys. Status Solidi A* **51**, 291 (1979).

⁸ M. S. Blanter and A. G. Khachaturyan, *Phys. Status Solidi A* **60**, 641 (1980).

⁹ V. A. Somenkov and S. S. Schilschtein, *Prog. Mater. Sci.* **24**, (3/4), 267 (1979).

¹⁰ A. S. Nowick and B. S. Berry, *Anelastic Relaxation in Crystalline Solids* (Academic, New York, 1972).

¹¹ M. S. Blanter *et al.*, *The Method of Internal Friction in Metallurgical Research* (Metallurgia, Moscow, 1991) (in Russian).

¹² M. S. Blanter and M. Ya. Fradkov, *Acta Met. Mat.* **40**, 220

(1992).

¹³ M. S. Blanter, *Phys. Status Solidi A* **133**, 317 (1992).

¹⁴ R. Kirchheim and E. Fromm, *Acta Metall.* **22**, 1397 (1974).

¹⁵ H. Peisl, in *Hydrogen in Metals*, edited by G. Alefeld and J. Völkl (Springer-Verlag, New York, 1978), Vol. 1.

¹⁶ H. Indrawirawan, O. Buck, and O. N. Carlson, *Phys. Status Solidi A*, **104**, 443 (1987).

¹⁷ J. Völkl and G. Alefeld, in *Hydrogen in Metals*, edited by G. Alefeld and J. Völkl (Springer-Verlag, New York, 1978), Vol. 1.

¹⁸ R. Hanada, M. Shinohara, Y. Sado, and H. Kimura, *J. Phys. (Paris) Colloq.* **42**, C5-757 (1981).

¹⁹ P. Schiller and H. Nijman, *Phys. Status Solidi A* **31**, K77 (1975).

²⁰ G. Cannelli and L. Verdini, *Ric. Sci.* **36**, 98 (1966).

²¹ P. Schiller and A. Schneiders, *Phys. Status Solidi A* **29**, 375 (1975).

²² S. Okuda *et al.*, *Acta Metall.* **32**, 2125 (1984).

²³ San-Qiang Shi and W. B. Li, *J. Phys. (Paris) Colloq.* **46**, C10-91 (1985).

²⁴ T. Ebata, R. Hanada, and H. Kimura, *J. Jpn. Inst. Met.* **55**, 29 (1991).

²⁵ G. Cannelli and L. Verdini, *Ric. Sci.* **36**, 246 (1966).